

Effect of Support Acidity on *n*-heptane Reforming over Pt/Beta zeolite+ γ Alumina Catalysts

Sergio Ramírez, Persi Schacht, Jorge Ancheyta

Instituto Mexicano del Petróleo, Eje Central Lázaro Cárdenas No. 152, México D.F. 07730, México, E-mail: sramire@imp.mx

Recibido el 18 de octubre del 2004; aceptado el 27 de mayo del 2005

Abstract. Platinum supported on beta zeolite+gamma alumina catalysts were synthesized in this work. The catalysts were prepared with Pt supported on mixtures of beta zeolite and alumina with different contents of zeolite in the final support, and with beta zeolite previously exchanged with lithium and cesium cations and mixed with alumina. Supports and catalysts were characterized by atomic absorption spectrometry, X-ray diffraction, nitrogen adsorption, FTIR of pyridine and CO adsorption, hydrogen chemisorption and NH₃ TPD. Results of supports characterization show values between the properties of raw materials and reveal that they have a uniform composition without destruction of the crystalline structures of beta zeolite and alumina. Activity of catalysts was evaluated in a glass reactor at 663 K and atmospheric pressure. Reforming of n-heptane was used as reaction test. Variations in the products selectivity of platinum supported catalysts were related to the composition of the support and the neutralization of the zeolite. These variations were attributed to the modification in the electronic properties of the supported platinum that affects the force and duration of the adsorbed hydrocarbon bond. The CO adsorption FTIR spectra also suggest the possibility of modifications in the morphology of the particles of supported platinum that may contribute to the changes in product selectivity.

Keywords: Beta zeolite, alumina, reforming, lithium, cesium

Introduction

Acid supports and their catalytic applications are of great interest for petroleum refining industry. The use of these materials opens a wide horizon of solutions to old problems associated to conventional catalysts [1,2]. One of the best examples is the application of zeolites as supports for reforming catalysts [3,4].

Reforming of hydrocarbons using different zeolites modified with alkaline cations has been subject of many investigations. The first studies were developed on Y-type zeolites, ZSM-5 [5,6,7] and beta zeolite [8,9]. To design these materials, researchers have taken as reference some characteristics of commercial catalysts (platinum supported on gamma alumina), such as the use of noble metal. Most of the efforts have been concentrated on the possibility of controlling the catalyst acid function by modifying zeolite acidity [10]. However, due to the specific properties of zeolites, the catalytic properties of supported platinum have been modified compared with those observed in traditional catalysts [11,12]. This modification has changed product selectivity during reforming reactions.

The changes in product selectivity with platinum supported on zeolites and on other solids have been extensively studied by means of FTIR of adsorbed molecules [13,14,15]. Results of FTIR of CO adsorbed on platinum have shown

Resumen. En el presente trabajo se prepararon muestras de catalizadores de platino soportadas en mezclas de zeolita beta+gama alúmina. Los catalizadores se sintetizaron utilizando diferentes contenidos de zeolita en el soporte final, así como empleando zeolita previamente intercambiada con cationes de litio y cesio, y mezclada con alúmina. Los soportes y los catalizadores se caracterizaron por absorción atómica, difracción de rayos X, adsorción de nitrógeno, FTIR de la adsorción de piridina y CO, quimisorción de hidrógeno y TPD de amoníaco. Los resultados de la caracterización de los soportes muestran propiedades con valores entre las de los materiales iniciales y revelan una composición uniforme sin destrucción de las estructuras cristalinas de la zeolita beta y la alúmina. La actividad catalítica de los catalizadores se evaluó en un reactor de vidrio a 663 K y presión atmosférica. Se utilizó la reformación de n-heptano como reacción de prueba. Las variaciones en la selectividad de los productos con la composición del soporte se correlacionaron con el grado de neutralización de la zeolita. Estas variaciones se atribuyeron a la modificación de las propiedades electrónicas del platino soportado que afectan la fuerza y la duración del enlace del hidrocarburo adsorbido. Los espectros FTIR de la adsorción de CO también sugieren la posibilidad de que las modificaciones en la morfología de las partículas de platino contribuyan a los cambios de selectividad observados.

Palabras clave: zeolita beta, alúmina, reformación, litio, cesio

shifts in the peaks of CO linearly adsorbed. Bezoukhanova et al. [14] found that CO stretching frequency for linear Pt-CO depends upon the nature of the alkali cation exchanged in L zeolite and interpreted these results in terms of the electric charge of the platinum particle. These researchers have established that the band at 2075-2090 cm⁻¹ can be ascribed to adsorbed CO on large particles typically at the external surface of zeolite.

A. de Mallmann and Barthomeuf [15] reported that metal particles are located in the supercages of the zeolite or in the net sodalita based on the frequency of the observed peaks of absorption. They have concluded that these changes affect zeolite morphology and catalytic activity. Siffert et al. [16] used XPS results to demonstrate that an increase of the electronic shift is observed when the basicity of the support is also increased and this modifies the reaction pathways of hydrocarbons adsorbed on platinum.

These observations have been attributed to two factors [17]: (1) the change of platinum electronic properties due to back-donation of electrons affecting the bond and selectivity of adsorbed species [16, 18], and (2) the modification on morphology and location of particles of supported platinum [14].

Although most of the above mentioned studies have been carried out on platinum supported on zeolites exchanged with alkaline metals, the use of the platinum supported on zeolites

mixed with alumina has not received too much attention. Recently, Kinger [19] reported that the mixture of MCM 41 and beta zeolite shows better transport properties in the n-heptane hydroisomerization compared with simple Pt supported on zeolite. Lately, Espinosa et al. [20] studied the reforming of n-heptane over Pt supported on mixtures of beta zeolite+alumina. They found an increase in hydrocracking when zeolite is added to alumina support. They also concluded that alumina becomes an inert material in this system.

In this work we explore the synthesis of binary supports of beta zeolite+alumina in order to take advantage of the structural and acid properties of both materials during reforming reactions. The main objective of our present investigation is to characterize the catalytic properties of the platinum by varying the acidity of the support and to correlate these properties with product selectivity in reforming of *n*-heptane.

Experimental

Preparation of the supports

Two series of platinum catalysts supported on beta zeolite (ZB) + alumina (AL) were synthesized. For the first series, supports were prepared with theoretical zeolite concentrations of 100, 35, 10 and 0 wt%. These supports were labeled as ZB100, ZB35, ZB10, and ZB0, respectively. The numbers indicate the zeolite content as weight percent of the solid. The second series of catalysts were supported on beta zeolite with and without neutralization with alkaline cations. For this series, the following three samples were prepared with 10 wt% of beta zeolite in the final support: ZB10 (without cations), ZB10Li (with 0.33 wt % of Li), ZB10Cs (with 6.44 wt % of Cs). The zeolite of these samples was previously exchanged with lithium and cesium cations using a procedure described elsewhere [21].

The weight percentage of cations corresponds to 100 % exchange considering a Si/Al molar ratio of the zeolite of 33.

All supports were prepared by integration of commercial beta zeolite (Zeolyst ZD97043) with Catapal B boehmite. Boehmite phase was transformed to gamma alumina by means of thermal treatment according to the following procedure: zeolite and boehmite powders were blended each one separately with water. Later, they were mixed and a small amount of nitric acid (0.1 M) was added as peptizant agent. The resulting solids were mixed vigorously and extruded with a plastic syringe in order to have a uniform size during the integration of platinum. The extrudates (3.2 mm diameter) were maintained at room temperature overnight. The prepared solids were dried 2 h at 313 K and later 2 h at 393 K. Finally, the solids were calcined at 823 K for 4 hours.

Integration of Platinum

The integration of platinum was performed by means of ion exchange method. Platinum II acetyl acetone (Aldrich)

diluted with toluene was used as platinum source in the alumina containing samples. The support was dried carefully at 623 K during 4 h for moisture elimination. The exchange solution was prepared with toluene previously dehydrated. The exchange was made in a closed recipient with magnetic agitation overnight. For the ZB100 sample $\text{Pt}(\text{NH}_3)_4(\text{NO}_3)_2$ (Aldrich) was used in aqueous solution due to its better metallic dispersion [22]. The catalysts prepared by this way were dried during 2 h at 313 K, 2 h at 393 K and calcined at 823 K for 4 hours in a furnace. The theoretical content of platinum was set at 0.4 wt %.

Characterization

The prepared materials were characterized by atomic absorption spectrometry (AAS), X-ray diffraction (XRD), nitrogen adsorption (BET), hydrogen chemisorption, NH_3 TPD and FTIR of pyridine and CO adsorbed.

Atomic absorption analyses were performed in a Perkin Elmer spectrometer 2380 model. AAS results and Si/Al molar ratio in the zeolite were employed to calculate the final content of zeolite in the binary supports (ZB+AL). The same procedure was used for determining lithium and cesium contents in the exchanged zeolite as well as platinum content in the final catalyst.

XRD spectra of beta zeolite+alumina supports were obtained with a Siemens D-5000 diffractometer equipped with a radiation monochromator $\text{CuK}\alpha$. Specific areas were determined with an ASAP sorptometer 2000 using the five points BET method.

The calculation of metal particle size was performed in a volumetric free of grease equipment by means of hydrogen chemisorption at room temperature on the catalyst previously reduced (723 K, 2 h) and degasified at high vacuum (10^{-6} Torr).

The determination of the number of acid sites of supports was made by means of anhydrous ammonia TPD. The samples deposited in a glass reactor were heated with helium flow from room temperature up to 823 K and maintained at this temperature during one and a half hour. Then, the samples were cooled down to 473 K and pulses of ammonia were added until the solid was saturated. After that, desorption of ammonia is started by heating at constant rate and the amount of desorbed ammonia is measured as a function of reactor temperature. The determination of desorbed ammonia was made with a Gow Mac Series 580 chromatograph fitted with thermal conductivity detector.

FTIR of pyridine and CO adsorption were obtained in a Nicolet 170 SX spectrometer. Briefly, the analysis is carried out as follows: the selfsupported wafers are introduced in a glass pyrex cell with CaF_2 windows and pretreated at high vacuum (10^{-6} Torr) and 673 K for 1 hour. Pyridine adsorption is carried out at room temperature by 30 minutes. The spectra of the adsorbed pyridine were recorded from room temperature to 773 K. The integrated absorbance of the bands at 1545 cm^{-1} (Brønsted) and 1450 cm^{-1} (Lewis) were considered for

acidity determinations using the transmission coefficients reported by Emeis [23]. The spectra of CO are recorded at room temperature on the reduced samples *in situ*. The self-supported wafers were treated with hydrogen overnight at 723 K.

Catalytic activity

Catalytic activity experiments were conducted at 663 K and atmospheric pressure in a glass reactor (0.6 cm ID). Reforming of *n*-heptane was chosen as reaction test. In a typical test 7 mg of catalyst and 93 mg of alpha alumina were loaded to the reactor. Alpha alumina inert material was used as catalyst diluent. *n*-heptane was fed to the reactor together with hydrogen in order to have a H₂/*n*-heptane molar ratio of 50.5. Prior to feeding *n*-heptane, the catalysts were reduced with electrolytic hydrogen at 723 K during 2 hours.

The identification of the products was carried out with a Varian 3400 CX gas chromatograph coupled with a flame ionization detector and a column of 60 m length and 0.13 mm ID applying a temperature program.

Selectivity of aromatics, isomers and hydrocracked products were calculated by dividing the corresponding yields by *n*-heptane conversion. Hydrocracking is considered as the yield of hydrocarbons with less than seven atoms of carbon (C₆⁻).

Results and Discussion

Characterization of support and catalyst

a) X-Ray Diffraction

Figure 1 shows the X-ray diffraction patterns of the first series of supports (ZB0, ZB10, ZB35, and ZB100). Progressive variations in intensity of the peaks of each material are observed as function of beta zeolite and alumina concentrations. This means that crystalline structures of each support are present,

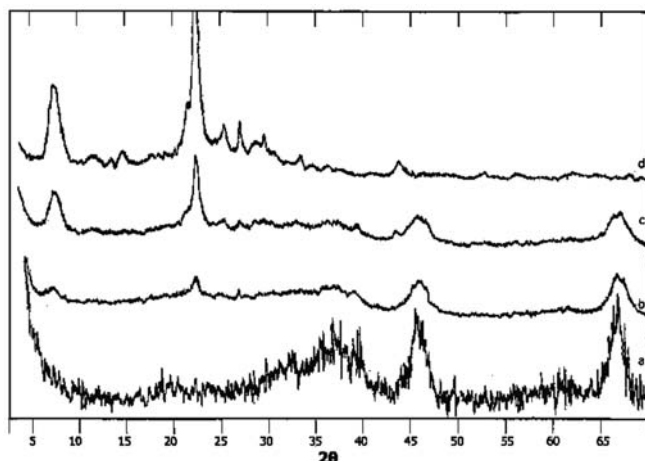


Fig. 1. X-ray diffraction patterns of beta zeolite+alumina supports. (a) ZB0, (b) ZB10, (c) ZB35, (d) ZB100.

and hence a uniform global concentration of these structures in the final solid can be assumed.

Supports made with alumina and beta zeolite exchanged with Li or Ce (spectra not shown) exhibit the same XRD pattern than ZB10 sample, which corresponds to the spectrum "b" in Figure 1. This similarity in XRD patterns is due to the same amount of beta zeolite (10 wt%) in supports with and without cations.

b) Atomic Absorption Spectrometry

Table 1 shows the characterization of the two series of supports and catalysts. Experimental contents of zeolite and platinum determined by AAS are presented in columns 2 and 9 respectively, which are very close to the expected values.

c) Nitrogen Adsorption

Specific areas (SA) of the first series of supports exhibited values between those found in zeolite (560 m²/g) and alumina (219 m²/g) pure samples. SA values of binary supports are in good agreement with those calculated with SA and the percentage of each material in the mixed support (338 vs 350 m²/g for the ZB35 sample and 253 vs 254 m²/g for the ZB10 sample). This similarity between calculated and experimental SA values confirms that the prepared supports are homogeneous mixtures of the two crystalline materials.

The addition of cations (Li or Cs) to the zeolite (second series of supports) reduced the specific area in about 10-13% with respect to ZB10 non exchanged sample. This behavior can be attributed to mechanisms of channels blockage of crystalline framework. The reduction in SA when Cs cation was added was bigger than Li due to the bigger amount and size of the former. We have found the same behavior in previous investigations [21]. In addition, ZB10Li sample has only 0.33 wt % of Li whereas the ZB10Cs sample has 6.44 wt % of Cs.

d) Hydrogen Chemisorption

Results of metallic dispersion obtained by hydrogen chemisorption showed very similar values for the first series of catalysts. The values vary between 70 and 75 %. The samples prepared with exchanged zeolite (second series) show platinum dispersion of 56 and 82 % for ZB10Li and ZB10Cs, respectively.

The platinum particle size in the first series of catalysts varies in the range of 12.7 to 13.3 Å. In the second series the biggest size of particles corresponds to ZB10Li sample, 19.6 Å. With these numbers it is less probable that most of the platinum particles are located inside the channels of zeolite.

e) Ammonia TPD

Population of acid sites of supports obtained by NH₃ TPD analysis is also shown in Table 1. All values are referred to the more acidic material (ZB100). In the first series of supports a decrease of acidity is observed when reducing the zeolite content in the support. ZB0 sample does not follow this trend which is due to its high population of Lewis sites corresponding to alumina. For the second series, very similar val-

Table 1. Properties of supports and catalysts

Sample	Supports						Catalysts		
	Zeolite wt%	SA m ² /g	Acid sites ^a	Brønsted sites ^{a,b}	Brønsted sites ^{a,c}	Lewis sites ^{a,c}	Disp. %	Pt wt%	Pt particle size, Å
Series 1									
ZB0	0.0	219	0.80	0.0	0.0	1.91	75	0.40	13.3
ZB10	12.8	254	0.76	0.0	0.0	1.38	70	0.37	13.2
ZB35	37.5	350	0.93	0.44	0.0	0.97	73	0.37	12.7
ZB100	100	560	1.00	1.00	1.00	1.00	75	0.39	13.0
Series 2									
ZB10	12.8	254	0.76	0.0	0.0	1.38	70	0.37	13.2
ZB10Li	10.0	230	0.77	0.0	0.0	1.0	56	0.44	19.6
ZB10Cs	8.2	220	0.72	0.0	0.0	0.34	82	0.39	11.9

^aReferred to ZB100 catalyst, ^bat 473 K, ^cat 673 K

ues of acid sites were obtained, which is mainly due to the following reasons: (1) the neutralization effect of cations when decreasing the Brønsted sites of the zeolite, (2) the Brønsted sites of zeolite are numerically much smaller than Lewis sites of alumina, therefore the cation exchange modifies only slightly the total acidity.

The thermograms of support ammonia desorption are shown in Figure 2. A decrease in the temperature of maximum peak is observed when zeolite concentration is reduced. This reveals that zeolite acid sites are stronger than alumina ones. The thermograms of ammonia desorption of catalysts (not shown) are more spread curves compared with those corresponding to each one of the supports without metal. Some authors [24] have suggested that this behavior is due to the regeneration of some Brønsted acidic sites by means of platinum reduction with hydrogen. Because we did not observe an increase in Brønsted acid sites population, we assume that

metallic platinum can act as weak Lewis acid site. The samples exchanged with lithium and cesium cations also showed a decrease in the peak of maximum desorption, which is a consequence of the neutralization of the protons associated to the structure of the acid zeolite. The decrease was higher with cesium due to its bigger electropositive nature.

f) FTIR of Pyridine Adsorption

The results of FTIR of pyridine adsorption show that the population of Brønsted acid sites in all supports is null at 673 K, except for ZB100 sample. At 473 K the ZB35 sample has less than one half of the Brønsted acidity of the ZB100 sample. For the first series, the dilution of zeolite acid sites when increasing the amount of alumina may be the reason for exhibiting this behavior. In the second series (10 wt % of zeolite) Brønsted acid sites were previously neutralized by means of lithium and cesium exchange before the zeolite was mixed with alumina.

The results of Lewis sites content show different behavior. It can be observed from Table 1 that Lewis sites increase as alumina content is also incremented, which is due to the high population of Lewis sites of this latter material. The effect of the cations exchange on the population of Lewis acid sites is not clear, since they do not exchange with this type of sites. The observed differences might be explained by the electropositive nature of lithium and cesium cations.

The results of FTIR in the region of the OH groups are shown in Figure 3. It is possible to distinguish the following OH groups associated to zeolite framework: 3740 cm⁻¹ for SiOH terminal, 3610 cm⁻¹ for SiAlOH bridged, and 3668 cm⁻¹ for Al extra framework. A decrease in the intensity of these peaks as direct function of zeolite content in the catalyst is observed. For the ZB0 sample these peaks are completely dispersed. This phenomenon is associated to the reduction in population of OH groups which contributes in some degree to Brønsted acidity of the material. The decrease of population

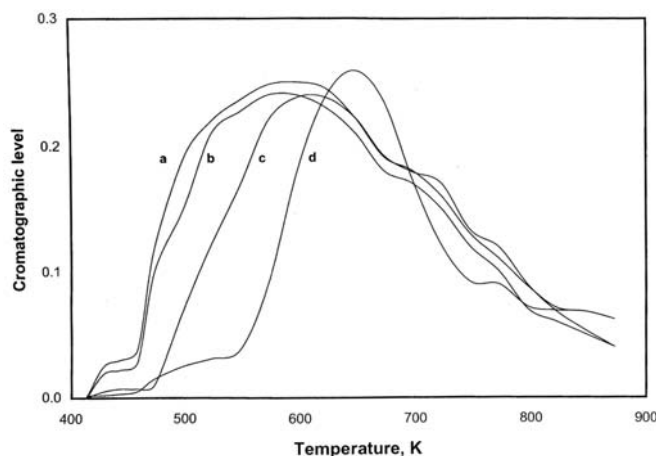


Fig. 2. Profiles of ammonia desorption in the first series of supports. (a) ZB0, (b) ZB10, (c) ZB35, (d) ZB100.

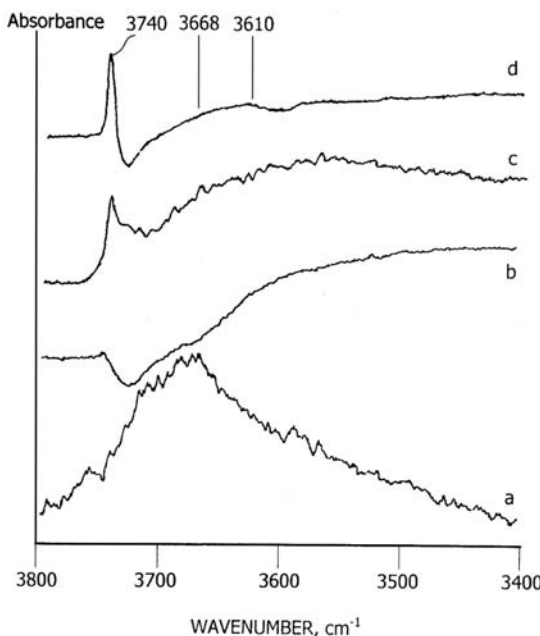


Fig. 3. Room temperature FTIR spectra of catalysts in the region of the hydroxil groups. (a) ZB0, (b) ZB10, (c) ZB35, (d) ZB100.

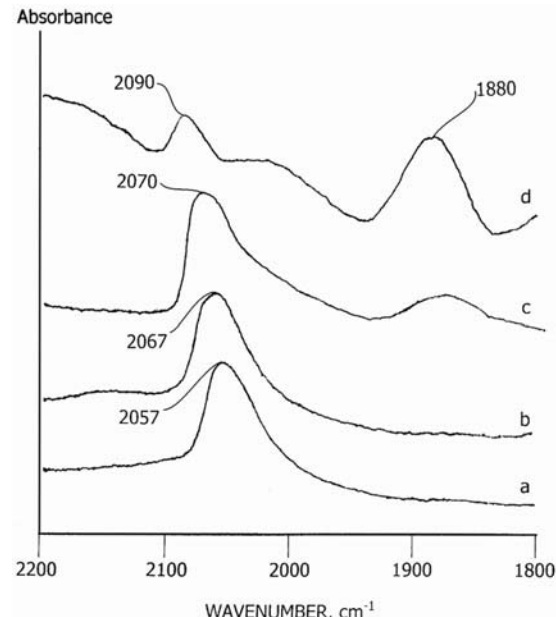


Fig. 4. Room temperature FTIR spectra of CO adsorption of catalysts in the region of high frequency. (a) ZB0, (b) ZB10, (c) ZB35, (d) ZB100.

can be explained by the dilution of these groups in the solid as the alumina content is increased or by the increase of the degree of protons exchanged by alkaline cations (for samples exchanged with lithium and cesium cations) [15].

g) FTIR of CO Adsorption

Figure 4 shows FTIR spectra of CO adsorption of the first series of catalysts. The peaks show a decrease in the vibration frequency of CO adsorbed linearly with the following trend: ZB100 > ZB35 > ZB10 > ZB0 (2090, 2070, 2067, 2057 cm⁻¹, respectively).

For all samples it is possible to observe a reduction in the wave number corresponding to the bands associated to CO linearly adsorbed on supported platinum as the zeolite content in the support becomes lower. These results suggest that electronic properties of supported platinum are modified as function of support nature. This type of modification has been explained as consequence of the increase in the electronic density of the metallic orbital d resulting in higher occupation of $2\pi^*$ orbital, which weakens the C=O bond [16]. The intensity of this peak is less pronounced in ZB100 and ZB35 samples.

The profile of the spectra corresponding to samples ZB100 and ZB35 shows the presence of both CO linearly adsorbed (2100-2000 cm⁻¹) and CO bridged adsorbed (1800-1900 cm⁻¹) bands, according to the assignation reported in the literature. Additional interpretations [14,18,25] have proposed that these results are associated to the morphology and nature (location) of the exposed metallic surface. It is also established that the lesser saturation degree (less number of neighboring atoms) the lesser stretching frequency. The ZB10 and

ZB0 samples show only one peak, and it is located in the region of CO linearly adsorbed. According to the platinum particle size shown in Table 1, our catalysts do not have platinum inside the channels of the zeolite; therefore we may suggest that there is an effect on the nature of platinum particles as function of the support nature.

The spectrum of CO absorption of the ZB100 sample shows a peak at 1880 cm⁻¹ which becomes less pronounced for ZB35 sample. In the former, the peak associated to CO linearly adsorbed is less intensive than the corresponding CO bridged adsorbed and is also shifted to high wave number. We can conclude that in addition to the influence of acidic properties of the support on the electronic properties of supported platinum, there is also an influence on the morphology and location of platinum particles. Our result seems to indicate that platinum particles in the samples with high zeolite content (ZB100 and ZB35) show both phenomena: modification of electronic properties of supported platinum and modification on morphology and location of platinum particles. As the zeolite content in the solid decreases, the spectrum shows the peak at 1880 cm⁻¹ less intensive with respect to high zeolite content samples, therefore platinum is also located on the alumina surface.

For the second series, the frequency of the peak varies from 2067 cm⁻¹ to 2024 cm⁻¹. The spectra of these samples do not present neither peaks of adsorption in the region of CO adsorbed in bridged form nor important variations among them, which could indicate that the effect of the modification of platinum electronic properties by the effect of support acidity is the only phenomenon present. Because cations are previ-

Table 2. Product Distribution, mol% ^a

Sample	Aromatics	Isomers	<i>n</i> -C ₇	Hydrocracked	TOF, molec/sit-s	<i>n</i> -C ₇ Conversion
Series 1						
ZB0	1.25	7.84	90.71	0.20	0.2	9.29
ZB10	2.11	11.09	80.80	6.00	0.8	19.20
ZB35	2.87	13.72	72.13	11.28	1.5	27.87
ZB100	18.4	1.50	24.80	55.30	4.3	75.20
Series 2						
ZB10	2.11	11.09	80.80	6.00	0.8	19.20
ZB10Li	1.90	9.00	88.30	0.80	0.9	11.70
ZB10Cs	1.50	7.10	90.70	0.70	0.5	9.30

^a Reaction conditions: 65 min time-on-stream, 663 K, atmospheric pressure, 50.5 H₂/n-heptane molar ratio.

ously exchanged in zeolite before mixing with alumina to produce the final support, we do not expect an interaction between platinum and the exchanged cations. The platinum crystals are too big to be located inside zeolite channels, where cations of lithium and cesium can be attached to zeolite framework.

Catalytic activity

The results of product distribution during catalytic activity tests of *n*-heptane reforming are shown in Table 2. Conversion of *n*-heptane, product yields and the number of converted molecules/metallic site-second (TOF) are reported as a function of zeolite content in the catalyst.

Products are lumped in aromatics (toluene), *n*-heptane isomers (2-methyl hexane, 3-methyl hexane, ethylcyclopentane, etc.), and hydrocracked products (C₆-). Non-converted *n*-heptane is also reported in Table 2.

a) First series of catalysts

In the first series, the highest TOF value corresponds to 100 % zeolite sample (ZB100). When *n*-heptane conversion is increased, TOF and hydrocracked products yield are also increased. Results of platinum content and dispersion showed in Table 1 indicate maximum differences of 13 % in all samples, however, the number of *n*-heptane converted by active site (TOF) varies by 20 times. These results indicate that the change in *n*-heptane conversion is not by far consequence of the differences in platinum content and dispersion.

Conversion and product distribution have a more or less lineal relationship with zeolite content. The acid sites population (zeolite concentration) seems to be the main responsible for the increase in *n*-heptane conversion.

Although we do not observe a major influence of platinum properties on the overall *n*-heptane conversion, a change in products selectivity is indeed observed. Figure 5 shows aromatics, isomers and hydrocracked product selectivities as

function of zeolite content. For aromatization reaction, the selectivity is in the following order: ZB0>ZB10≈ZB35<ZB100. The more important variation is observed in the ZB100 sample. Aromatics selectivity is almost one half when alumina (ZB0) is changed by zeolite (ZB100) as catalyst support. Isomers selectivity exhibits a more drastic behavior changing from 84.4 % in the catalyst supported on ZB0 to 2 % for the ZB100 supported catalyst.

The sample containing 100% alumina (ZB0) follows preferably the aromatization and isomerization pathways, its behavior corresponds to a bimetallic catalyst with weak acidic function. It is a low activity catalyst. It does not have Brønsted acid sites that promote isomerization and cyclization reactions that may lead to aromatics production. The sample with 100% beta zeolite (ZB100) produces preferably hydrocracked products. This latter sample showed the highest TOF value, which implies that the effect of acid properties of the support plays a predominant role. Platinum properties do not show important

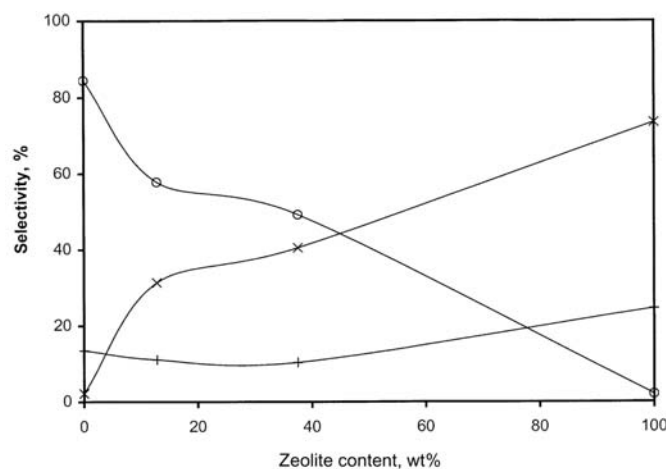


Fig. 5. Selectivity towards different hydrocarbons: (O) Isomers, (+) Aromatics, (X) Cracked products.

effects on catalytic activity. It does not matter if the metal is agglomerated or more or less active; or if the platinum particles have different morphology.

On the basis of these results, it can be stated that the pathway of the reaction is modified as the zeolite content is increased in the support. The main effect is the increased hydrocracking activity as function of zeolite content in the catalysts. The increment in population of Brønsted acid sites as the content of zeolite in the catalyst is increased is the main responsible of this behavior. A second effect is observed on platinum properties as a consequence of support properties. The modification of the FTIR of CO adsorbed spectra may indicate two different affecting factors: (1) modification of electronic properties of supported platinum, and (2) the changes on morphology of the platinum supported particles.

The behavior of the catalysts with high content of zeolite does not correspond to a bifunctional catalyst. It seems to be like monofunctional acidic catalyst. The mechanism for bifunctional catalysts is more complex and requires the participation of both, metallic and acid functions of catalyst [27]. In order to reach an equilibrium in the two functions of the catalyst it is necessary to take into account the platinum sites, dispersion and also the population and strength of acidic sites, all of them depend on the preparation method.

Our results are in good agreement with those reported by Espinosa et al. [20]. When catalyst support is changed from alumina to zeolite hydrocracking reaction increases by means of the population of strong acidic sites.

The shape of selectivity curves suggests that it is possible to adjust the alumina/zeolite ratio in the zeolite based on the desired conversion and selectivity. The samples with low zeolite content (ZB10, ZB35) show a more equilibrated acid metallic functions. They behave more likely as bifunctional catalyst [26].

b) Second series of catalysts

The samples exchanged with cations have the lowest hydrocracking activity compared with the sample without cations (ZB10). The highest TOF corresponds to the ZB10Li sample. Lithium in this sample controls hydrocracking level and it also maintains TOF activity.

Addition of lithium and cesium cations to zeolite decreases the acid sites population (strong Brønsted acid sites), and therefore, a reduction in concentration of hydrocracked products is observed. The products distribution is about the same for catalyst exchanged with both Li and Cesium cations. These catalysts behave as monofunctional catalyst with a very weak acid function and their results are comparable with those obtained with ZB0 catalysts. The interaction between platinum and cations is expected to be very weak [28].

Catalysts prepared with ZB10Li and ZB10Cs supports show lower aromatics (16.24, 16.13) selectivity and higher isomers (76.9, 76.34) selectivity than ZB100 sample (24.47 and 1.99), but with smaller hydrocracking levels (73.54 vs 6.84 and 7.523). The modification in selectivity of these catalysts with respect to ZB10 sample may be due to the support

acidity and to its effect on the modification of platinum electronic properties. It is probable that the modification in the morphology of platinum is not deep enough compared with ZB100 sample.

These changes in selectivity have been observed by different authors. Using XPS, Siffert et al. [16] detected an increase in the electronic shift from zeolite framework to the Pt particles when increasing basicity. The electronic shift between support and platinum particles produces changes in the enthalpy of adsorption of the hydrocarbon species, which would decrease when the basicity increases; this phenomenon is reflected as changes in reaction mechanism pathways.

Conclusions

Variations in conversion and products selectivity of platinum supported on mixtures of beta zeolite+alumina during reforming of *n*-heptane can be explained in terms of change of support acidity. Conversion and product yields have a lineal relationship with zeolite content. The acid sites population seems to be the main responsible for the increase in *n*-heptane conversion. These results indicate that the change in *n*-heptane conversion is not by far consequence of the differences in platinum and dispersion and morphology. However, spectra of FTIR of CO adsorption suggest that modifications in the morphology and location of the supported platinum particles can take place as consequence of support acidity.

Acknowledgments

The authors thank Instituto Mexicano del Petróleo for its financial support.

References

1. Moscou, L. *Stud. Surf. Sci. Catal.* **1991**, *58*, 1.
2. Chen, N. Y.; Degnan, T. F. *Chem. Eng. Prog.* **1988**, 32-41.
3. Tamm, P. W.; Mohr, D. H.; Wilson, C. R. in *Catalysis 1987* Ward, J. W., Ed. **1988**, 335-353.
4. Dessau, R. M.; Valyocsik, E. W. *US patent 4,882,040* **1989**.
5. Gallezot, P. *Catal. Rev.-Sci. Eng.* **1979**, *20*, 121-154.
6. Chester, W. *J. Catal.* **1984**, *86*, 16-23.
7. Dessau, R. M. *J. Catal.* **1984**, *89*, 520-526.
8. Martens, J. A.; Pérez-Pariente, J.; Jacobs, P. A. in: *Chemical Reactions in Organic and Inorganic Constrained Systems*, Setton, R., Ed., D. Reidel Publishing Company **1986**, 115-129.
9. Corma, A.; Fornés, V.; Heap, J. B.; Orchillés, A. V. *J. Catal.* **1987**, *107*, 288-295.
10. Hughes, T. R.; Buss, W. C.; Tamm, P. W.; Jacobson, R. L. *Proc. 7th Int. Conf. on Zeolites*, Tokyo **1986**, 725-732.
11. Ramírez, S.; Viniegra, M.; Domínguez, J.M.; Schacht, P.; De Ménorval, L. *Ch. Catal. Lett.* **2000**, *66*, 25-32.
12. Zheng, J.; Dong, J. L.; Xu, Q. H.; Liu, Y.; Yan, A. Z. *Appl. Catal. A* **1995**, *126*, 141-152.
13. Primet, M.; Basset, J. M.; Mathieu, M. V.; Prettre, M. *J. Catal.* **1973**, *29*, 213-223.

14. Besoukhanova, L.; Guidot, J.; Barthomeuf, D.; Breysse, M.; Bernard, J. R. *J. Chem. Soc. Faraday Trans.* **1981**, *77*, 1595.
15. De Mallman, A.; Barthomeuf, D. *Stud. Surf. Sci. Catal.* **1989**, *46*, 429-438.
16. Siffert, S.; Schmitt, J. L.; Sommer, J.; Garin, F. *J. Catal.* **1999**, *184*, 19-28.
17. Menacherry, P. V.; Haller, G. *J. Catal.* **1998**, *177*, 175-188.
18. Van Santen, R. A. *J. Chem. Soc. Faraday Trans. I* **1987**, *83*, 1915-1934.
19. Kinger, G.; Majda, D.; Vinek H. *Appl. Catal. A* **2002**, *225*, 301.
20. Espinosa, G.; Bautista, J. M.; Silva, H.; Muñoz, L.; Batina, N. *Appl. Catal. A* **2002**, *231*, 117-123.
21. Ramírez, S.; Domínguez, J.M; Viniegra, M.; De Ménorval, L. *Ch. New J. Chem.* **2000**, *24*, 99-104.
22. Kouwenhoven, H. W.; De Kroes, B. *Stud. Surf. Sci. Catal.* **1991**, *58*, 497.
23. Emeis, C. A. *J. Catal.* **1993**, *141*, 347-354.
24. Ostgard, D. J.; Kustov, L.; Poeppelmeier, K. R.; Sachtler, W. M. H. *J. Catal.* **1992**, *133*, 342-357.
25. Jacobs, G.; Alvarez, W. E.; Resasco, D. E. *Appl. Catal. A* **2001**, *206*, 267-282.
26. Lugstein, A.; Jentys, A.; Vinek, H. *Appl. Catal. A* **1998**, *116*, 29-38.
27. Pellet, R. *J. J. Catal.* **1998**, *177*, 40-52.
28. Norcross, J. A.; Slichter, Ch. P.; Sinfelt, J. H. *Catal. Today* **1999**, *53*, 343-356.